SCANNING VOL. 9999, 1–8 (2016)

Scanning Electron Microscopy Combined With Image Processing Technique: Analysis of Microstructure, Texture and Tenderness in *Semitendinous* and *Gluteus Medius* Bovine Muscles

Facundo Pieniazek[1] and Valeria Messina[1,2]

[1]CINSO—UNIDEF (Strategic I & D for Defense)—MINDEF-CITEDEF-CONICET, Villa Martelli, Buenos Aires, Argentina
[2]The National Council for Scientific and Technical Research (CONICET), Rivadavia, Buenos Aires, Argentina

Summary: In this study the effect of freeze drying on the microstructure, texture, and tenderness of *Semitendinous* and *Gluteus Medius* bovine muscles were analyzed applying Scanning Electron Microscopy combined with image analysis. Samples were analyzed by Scanning Electron Microscopy at different magnifications (250, 500, and 1,000×). Texture parameters were analyzed by Texture analyzer and by image analysis. Tenderness by Warner–Bratzler shear force. Significant differences ($p < 0.05$) were obtained for image and instrumental texture features. A linear trend with a linear correlation was applied for instrumental and image features. Image texture features calculated from Gray Level Co-occurrence Matrix (homogeneity, contrast, entropy, correlation and energy) at 1,000× in both muscles had high correlations with instrumental features (chewiness, hardness, cohesiveness, and springiness). Tenderness showed a positive correlation in both muscles with image features (energy and homogeneity). Combing Scanning Electron Microscopy with image analysis can be a useful tool to analyze quality parameters in meat. Summary SCANNING 9999:1–8, 2016. © 2016 Wiley Periodicals, Inc.

Key words: muscle, image analysis, scanning electron microscopy, surface analysis

Abbreviations

ASM	energy
C	cooked
CFD	cooked freeze dried
CFDR	cooked freeze-dried rehydrated
CHEW	chewiness
COH	cohesiveness
CON	contrast
COR	correlation
ENT	entropy
GLCM	gray level co-occurrence matrix method
GM	*Gluteus Medius*
HAR	hardness
HOM	homogeneity
PCA	principal component analysis
RES	resilience
SEM	scanning electron microscopy
SPRIN	springiness
ST	*Semitendinous*
WBSF	Warner–Bratzler shear force measurement

Introduction

Meat is a widely consumed product; it is also a perishable product. In order to enhance its quality, new techniques are continuously developed and at the same time, novel techniques are required for its efficient and effective quality measurement and control.

Texture in food has been defined as "all the rheological and structural (geometric and surface) attributes of the product perceptible by means of mechanical, tactile, and where appropriate, visual and auditory receptors" (Lawless and Heymann, '98). Texture parameters are usually measured by conventional techniques, such as sensory and instrumental methods, which are time consuming and destructive to the product. The relationship of instrumental texture variables to the human perception of texture has been a very active area of research, with many researchers addressing this topic (Guzek *et al*., 2013; Luckett *et al*., 2014).

Conflict of interest: None.

Address for reprints: Valeria Messina, The National Council for Scientific and Technical Research (CONICET), Rivadavia 1917, Buenos Aires C1033AAJ, Argentina
E-mail: vmessina@citedef.gob.ar

Received 3 February 2016; Accepted with revision 31 March 2016

DOI: 10.1002/sca.21321
Published online XX Month Year in Wiley Online Library (wileyonlinelibrary.com).

Multiple instrumental methods have been developed in an attempt to assess the texture of meats, with a focus on the "tenderness" of whole muscle meat products (Chen and Opara, 2013; Wezemael *et al*., 2014). Among many quality parameters, tenderness is regarded as one of the most important attributes that affects the eating quality of meat. It is positively correlated with juiciness and taste and it has a substantial influence on overall customer satisfaction (Rust *et al*., 2008; Juarez *et al*., 2012).

An interesting alternative for analyzing the surface of food products and quantifying appearance characteristics is to use computerized image analysis techniques (Mendoza *et al*., 2012; Saini *et al*., 2014). Image analysis can be a useful tool for characterizing food morphology because the highly irregular structures of many food materials elude precise quantification by conventional means. This technique allows obtaining measurements from digitalized images providing objective evaluations of the morpho-colorimetric features of samples, a method that is more quantitative and less biased than the common method of visual perception, which is prone to variation due to the personal opinions of inspectors or trained panels (Kono *et al*., 2014). When microscopy techniques such as scanning electron microscopy (SEM) and images analysis are used together, they become a powerful tool to evaluate microstructure changes of a product; cell size and number of cells can them be measured and quantified from the projected image. Employing image processing with SEM, some important sensory attributes such as texture, tenderness among others, could be predicted by processing the surface and cross section images of a product.

The aim of the present research was to study the effect of freeze drying on the microstructure, texture and tenderness of *Semitendinous* and *Gluteus Medius* bovine muscles for instant meal applying image analysis techniques on SEM micrographs performed at different magnifications. Data obtained by image analysis was correlated with instrumental analysis in order to evaluate effectiveness of the method.

Material and Methods

Samples, Cooking Process, and Freeze Drying Cycle

Semitendinous (ST) (n = 4) and *Gluteus Medius* (GM) (n = 4) sp: Aberdeen Angus bovine muscles were provided by an abattoir center of Argentina. Preliminary experiments were conducted to test different operative conditions such as: sample shape, dimension and thickness, method, time of cooking, various procedures to manipulate the sample and freeze drying cycle. The best operating conditions were: whole muscles were cut to about $4 \times 2 \times 2$ cm steaks with the fiber parallel to the longest axis and were individually labeled and weighed. Steaks were grilled in aluminum-folded strips and cooked to an end point temperature of $71.5 \pm 0.5^{\circ}$C (AMSA, 1995) using an electric grill (Philips, CABA, Argentina). Internal temperature was monitored with a T-type thermocouple inserted in the geometric center of each steak. Samples were cooled at room temperature (30 min) and then chilled in a refrigerator at $4 \pm 1^{\circ}$C for 24 h.

Each cooked (C) steak was cut with a cork-bore to a cylindrical form with 13 mm diameter and 3 cm high. The round shape was the best solution to reduce variability caused by lateral sinking. Each cylindrical sample were sliced in units of 1 mm of thickness and stored at 3°C until freeze drying process.

Freeze drying process was carried out in a pilot plant freeze dryer supplied with four trays designed by an Industrial constructor (Rificor, Buenos Aires, Argentina). Freeze drying cycle was set at −50 during 24 h and then dried at 40°C during 48 h under a chamber pressure of 0.346 Pa. Samples were packaged, individually identified and stored in a dark place at room temperature until analysis.

In order to analyze microstructure, instrumental and image texture features of cooked freeze-dried rehydrated samples (CFDR), rehydration was performed with tap water at 98°C. The duration of rehydration process in both muscles was fixed in 6 min, as after that time period there was no more absorption of water by the samples.

Scanning Electron Microscopy

Scanning Electron Microscopy was used for the observation of the microstructure of cooked freeze dried (CFD) and cooked freeze dried rehydrated samples of ST and GM. Samples were cross sectioned using a scalpel; the cut was always performed in the same direction. Samples were mounted on holders and coated with gold (Messina *et al*., 2014). Microscopic evaluation was performed using a Scanning Electron Microscope (SEM 515, Philips, Amsterdam, Netherland). Observations of the samples at magnification of 250, 500, and 1,000× were obtained for image analysis (Model Genesis Version 5.21).

Brightness and contrast are the most important variables that must be controlled during the acquisition of images; therefore, the values of these parameters were kept constant for each magnification during the process of image acquisition.

Textural Profile Analysis (TPA)

Textural profile analysis of CST, CGM, CFDRST, and CFDRGM was measured individually using a Texture Analyzer (TA-XT-Texture Technologies,

Corp., UK) with a 5 kg load cell using a two-cycle compression method. Samples were compressed 3 mm with a time interval of 5 s at a speed of 5.0 mm s^{-1}. Results were reported as an average value. Hardness (HAR) was determined from the first test curve. Cohesiveness (COH), springiness (SPRIN), chewiness (CHEW), and resilience (RES) were also determined. Samples were analyzed trice.

Image Texture Analysis

Image analysis was measured at different magnifications 250, 500, and 1,000× of CST, CGM, CFDRST, and CFDRGM, respectively. Eighteen images of $1{,}024 \times 800$ pixels were captured using an Scanning Electron Microscopy and stored as bitmaps in a gray scale with brightness values between 0 and 255 for each pixel constituting the image. The size of each sample (region of interest: 122×122 pixels) was the same for all the evaluated magnifications.

Texture parameters (energy [ASM], contrast [CON], correlation [COR], homogeneity [HOM], and entropy [ENT]) were calculated on SEM images using the gray level co-occurrence matrix method (GLCM).

The textural feature angular second moment also called ASM, measures the texture uniformity or orderliness of an image (Ou *et al*., 2014). ASM values indicate more directional uniformity in the image (Yang *et al*., 2000). The textural feature CON is a measure of the intensity contrast between a pixel and its neighbor over the whole image. It measures the local variation in the GLCM. CON can be seen as dynamic range of gray level or sharpness of edges. The range of CON lies [0 (size(GLCM,1)−1)^2]. Furthermore, contrast is 0 for a constant image (Laddi *et al*., 2013).

The textural feature COR is a measure of how correlated a pixel is to its neighbor over the whole image. Its range lies between -1 and $+1$. Also, the correlation is $+1$ or -1 for a perfectly positively or negatively correlated image. Correlation measures the joint probability of occurrence of pixel pairs of GLCM. The textural feature ENT shows how often a pixel with gray-level (grayscale intensity) value i occurs horizontally adjacent to a pixel with the value j (Karimi *et al*., 2012). ENT is a statistical measure of randomness that can be used to characterize the texture of the input image. ENT is higher when all entries in p (i, j) are of similar magnitude and small when the entries in p (i, j) are unequal (Laddi *et al*., 2013). HOM shows the level of uniformity on the image. High values of HOM show improvement of uniformity and smoothness of the image.

Five image texture features (Correlation [COR], Energy [ASM], Homogeneity [HOM], Entropy [ENT], and Contrast [CON]) were calculated using MATLAB 8.4 (The MathWorks, Inc., MA) (Eqs. 1–5):

$$\mathrm{CON} = \sum_{i=0}^{n-1}\sum_{j=0}^{n-1} (i-j)^2 \mathrm{Pd},\theta(i,j) \tag{1}$$

$$\mathrm{ENT} = -\sum_{i=0}^{n-1}\sum_{j=0}^{n-1} \mathrm{Pd},\theta(i,j)^2 \mathrm{LogP}(i,j) \tag{2}$$

$$\mathrm{HOM} = \sum_{i=0}^{n-1}\sum_{j=0}^{n-1} \frac{\mathrm{Pd},\theta(i,j)}{1+|i-j|} \tag{3}$$

$$\mathrm{ASM} = \sum_{i=0}^{N-1}\sum_{j=0}^{N-1} \mathrm{Pd},\theta(i,j)^2 \tag{4}$$

$$\mathrm{COR} = \frac{\left[\sum_{i=0}^{N-1}\sum_{j=0}^{N-1} (ij)\mathrm{P}(i,j)\right] - \mu_x\mu_y}{\sigma_x\sigma_y} \tag{5}$$

WarnerBratzler Shear Force Measurement (WBSF)

Eight cores (1.27 cm diameters and 2.5 ± 0.2 cm in length) were obtained from each steak parallel to the muscle fiber's orientation for WBSF determination. The Warner–Bratzler shear test was performed using an Instron universal testing machine (Instron, Model 4301, Instron Ltd., UK) fitted with an inverted V shaped blade. The WBSF scores were obtained for all cores extracted from an individual sample and averaged the peak value of the shear force for each core for the tenderness reference value.

Statistical Analysis

Texture and WBSF values were subjected to linear normalization prior to Principal Component analysis (PCA) in order to efficiently suppress quantitative effects on the multivariate data. Mean values were compared by T-Student, regression equations and correlation coefficients (R^2) between instrumental and image texture features were obtained using SPSS-Advanced Statistics 12 software (SPSS Inc., Chicago, IL).

Results and Discussion

Scanning Electron Microscopy

Figure 1 shows microstructure at different magnifications (250, 500, and 1,000×) of CST, CFDST, and CFDRST and Figure 2 of CGM, CFDGM, and CFDRGM.

CST and CGM showed an organized structure with compacted fibers without gaps among fiber. CFDST

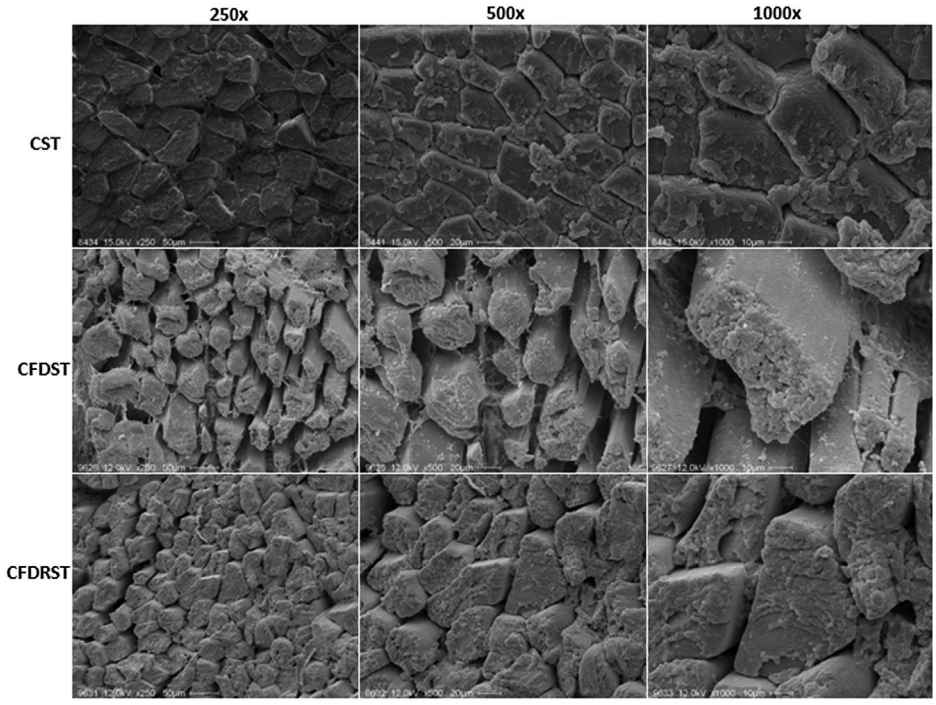

Fig 1. Scanning micrographs performed at 250, 500, and 1,000× of cross sectional cooked (C), cooked freeze dried (CFD), and cooked freeze dried rehydrated (CFDR) *Semitendinous* muscle (ST).

and CFDGM structures appeared organized showing gaps among fiber bundles and between fibers. Myofibrils were dehydrated and separated and partially fragmented. CFDST and CFDGM samples freezed at −50˚C showed a porous size structure with larger and irregular cavities due to ice crystals formed, CFDGM had higher porous size structure and shrinkage of fiber when compared to CFDST. Amount of pores (porosity) in samples depends on different factors like cooking parameters, pressure and drying

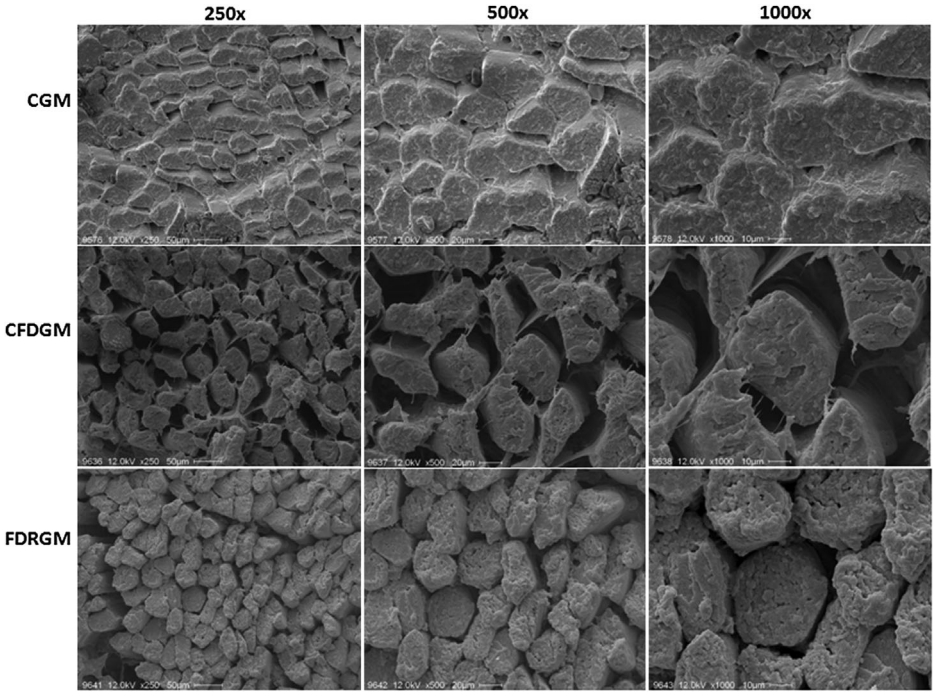

Fig 2. Scanning micrographs performed at 250, 500, and 1,000× of cross sectional cooked (C), cooked freeze dried (CFD), and cooked freeze dried rehydrated (CFDR) *Gluteus Medius* muscle (GM).

temperature. During subsequent freezing and freeze-drying the ice sublimation creates pores; the amount of pores (porosity) is related to the water uptake and is higher when the water uptake is increased. The porous structure is also influenced by the freezing process and a fast cooling with a high undercooling leads to smaller ice crystals and a larger inner surface. Due to the high porosity the freeze dried cell suspension has a high specific surface area; this influences the sorption behavior as well as the rehydration (Mounir, 2015).

Higher amounts of pores (higher porosity) help to maintain the structure without the deformations that are inevitable in other drying methods (Leelayuthsoontorn and Thipayarat, 2006). The degree of porosity also has influence in texture and rehydration ability, when the size of the air cells in porous material are bigger, it allows a fast rehydration due that water easily enters and reoccupies the empty spaces (Oikonomopoulou *et al*., 2011).

CFDRST and CFDRGM showed that porous size structure due to ice sublimation during freeze drying process, water easily reoccupied the empty spaces in all samples.

In general micrographs showed that changes in microstructure a probably due to that drying process induced faster denaturation of proteins and subsequently more reduction in dimension of myofibrils and collagen, resulting in shrinkage of muscle fiber diameter and sacromere length (Kong *et al*., 2008; Reyes *et al*., 2011).

Image Texture Analysis

Table I shows image texture values for CST, CGM, CFDRST, and CFDRGM at different magnification (250, 500, and 1,000×). In texture image analysis, COR indicates the linearity of the image. For an image with large areas of similar intensities, a high value of correlation is measured. HOM shows the level of uniformity on the image. High values of HOM show improvement of uniformity and smoothness of the image (Karimi *et al*., 2012). ENT is a measure of randomness, and takes low values for smooth images. ASM represents the smoothness of an image, when ASM is high the image has very similar pixels. CON is a measure that shows the difference from one pixel to others close to it. It is a measure of local gray variations (Zheng *et al*., 2006). Low values in CON represent diminish of local variation of pixels. The softer the texture the lower the contrast, which is due to lower pixel value difference between two neighbors.

CST and CFDRST at 250× magnification showed significant differences ($p < 0.05$) for ASM, CON, ENT, COR, and HOM; 500× for ENT; and 1,000× for ASM, CON, ENT, COR, and HOM. Higher values of HOM, COR, ASM and lower values of CON and ENT were obtained at 1,000×, showing that at higher magnification in SEM, images analysis showed to be homogeneous, a better correlation among neighboring pixel was obtained, lower degree of local variations appeared, and high linearity and smoothness was observed.

TABLE I Image texture values of cooked and cooked freeze dried rehydrated *Semitendinous* and *Gluteus Medius* bovine muscles (Sp: Aberdeen Angus) at different magnifications

		Image texture				
Sample	Magnification	ASM	ENT	CON	COR	HOM
CST	250×	0.33[a]	5.94[b]	0.47[a]	0.68[b]	0.88[a]
CFDST	250×	0.14 b	6.99[a]	0.26[b]	0.78[a]	0.8[b]
p-value		0.0001	0.0001	0.0001	0.0001	0.0053
CST	500×	0.22	6.30[b]	0.39	0.67	0.83
CFDRST	500×	0.21	6.51[a]	0.39	0.67	0.83
p-value		NS	0.0015	NS	NS	NS
CST	1,000×	0.29[b]	6.53[a]	0.70[a]	0.81[b]	0.91[b]
CFDRST	1,000×	0.70[a]	4.83[b]	0.23[b]	0.93[a]	0.94[a]
p-value		0.0001	0.0001	0.0001	0.0001	0.0001
CGM	250×	0.69[a]	6.68[a]	0.79[a]	0.16[b]	0.79[b]
CFDRGM	250×	0.23[b]	6.57[b]	0.33[b]	0.74[a]	0.85[a]
p-value		0.0001	0.0001	0.0001	0.0001	0.0001
CGM	500×	0.20[b]	6.35[b]	0.38[a]	0.77[a]	0.83[b]
CFDRGM	500×	0.28[a]	6.68[a]	0.26[b]	0.74[b]	0.88[a]
p-value		0.0001	0.0001	0.0001	0.0001	0.0001
CGM	1,000×	0.86[b]	6.80[a]	0.94[a]	0.92[b]	0.95[b]
CFDRGM	1,000×	0.99[a]	5.35[b]	0.88[b]	0.95[a]	0.97[a]
p-value		0.0056	0.0001	0.0001	0.0051	0.0054

NS, son significant; C, cooked; CFDR, cooked freeze dried rehydrated; ST, *Semitendinous*; GM, *Gluteus Medius*. Small letters in the same column indicate that means are significantly different ($p < 0.05$) related to treatment (T-student)

CGM and CFDRGM at 250, 500, and 1,000× magnification showed significant differences ($p < 0.05$) for ASM, CON, ENT, COR, and HOM. Higher values of HOM, COR, ASM, and lower values of CON and ENT were obtained at 1,000×.

CFDRST and CFDRGM showed lower values of CON, which is related to lower stickiness (Meullenet *et al*., '98). CFDST showed higher values of CON when compared to CFDRGM. Jeyamkondan *et al*. (2001) reported in bovine beef that when image texture features was evaluated at different magnifications, the use of magnified images increases prediction accuracy on texture features and reduces computation time.

Results revealed that CST, CGM, CFDRST, and CFDRGM had lower CON values revealing a lower degree of local variations which is typical of softer and more homogeneous surfaces; whereas high values of COR suggests strong correlation among neighboring pixel in an image, lower degree of local variations appeared, and high linearity and smoothness was observed at 1,000×.

Instrumental Texture Analysis

Table II shows texture values of cooked and cooked freeze dried rehydrated ST and GM. Statistical difference ($p < 0.05$) was obtained for CHEW, HARD, COH, and SPRIN in CST, CGM, CFDRST, and CFDRGM, respectively.

CFDRST and CFDRGM had higher texture values when compared to CST and CGM. In general, results revealed that higher values of HARD, SPRING, CHEW, and RES were obtained for GM samples when compared to ST.

Correlation Between Instrumental and Image Texture

In order to evaluate the capability of instrumental and image analysis for texture, a linear trend with a linear correlation under evaluated conditions were analyzed with instrumental features (CHEW, COH, SPRING, and HARD) versus image features (ASM, CON, ENT, COR, and HOM) in ST and GM.

PCA was performed for each texture parameters (instrumental and image). Two PC's were found for instrumental texture accounting 93.6% (ST) and 91.2% (GM) of the total variance and two PC's were found for image texture accounting 90.8% (ST) and 89.5 (GM) of the total variance. Each PC score was multiplied by the respective variance. PC_1 of instrumental and image texture were combined using a linear combination. Figure 3 shows linear trend with a linear correlation of PCA scores of texture parameters (instrumental vs. image texture). Results revealed a strong relationship between instrumental and image features for ST ($R = 0.946$) and GM ($R = 0.937$), based on the resulting R^2 value, the model explained 86.0% and 84.0%, respectively, of the variability that associated instrumental with image features.

TABLE II Instrumental texture values of cooked and cooked freeze dried rehydrated *Semitendinous* and *Gluteus Medius* bovine muscles (Sp: Aberdeen Angus)

	Instrumental texture				
Sample	HARD	SPRING	COH	CHEW	RES
CST	67.79[b]	0.44[b]	0.50[b]	16.72[b]	0.16
CFDRST	69.82[a]	0.47[a]	0.54[a]	17.89[a]	0.18
p-value	0.0001	0.0001	0.0001	0.0001	NS
CGM	71.35[b]	0.51[b]	0.49[b]	18.31[b]	0.19
CFDRGM	72.35[a]	0.55[a]	0.52[a]	19.10[a]	0.20
p-value	0.0001	0.0001	0.0001	0.0001	NS

NS, non significant; C, cooked; CFDR, cooked freeze dried rehydrated; ST, *Semitendinous*; GM, *Gluteus Medius*. Small letters in the same column indicate that means are significantly different ($p < 0.05$) related to treatment (T-student)

Image Texture Analysis and WBSF: Tenderness

Basset *et al*. (2000) stated that texture analysis could be extended to prediction of tenderness in meat, because the meat tissue characteristics that influence meat quality, and the connective tissue quantity and spatial distribution that define the grain of meat are directly related to tenderness. Some authors have reported that image texture features can be applied to evaluate tenderness and toughness in meat (Jackman *et al*., 2009; ElMasry *et al*., 2012; Sun *et al*., 2012; Jackman and Sun, 2013).

In previous studies Belew et al. (2003) and Sullivan and Calkins (2011) reported that threshold values for WBSF between 31.38 and 38.25 N were used as cut-off values for very tender and tender beef respectively. Based on WBSF threshold values reported by the stated authors mentioned above ($31.38\ N \leq X \geq 38.25\ N$), mean values of WBSF of cooked samples ($CST = 37.88$ N; $CGM = 33.15$ N) were higher than freeze dried rehydrated samples ($FDRST = 36.53$ N; $FDRGM = 31.89$ N). ST showed higher WBSF when compared to GM bovine muscle.

In order to correlate image texture features with WBSF; threshold values for WBSF between 31.0 and 39.0 N were used as cut-off values for very tender beef. Principal Component Analysis was applied for image texture features and WBSF data. Two PC's for ST muscles explaining 95.7% and 3.0% of the total variance (98.7%) was obtained and two PC's for GM, 93.5% and 4.1% of the total variance (97.6%; data non shown). Results revealed that ASM and HOM were positively correlated with WBSF ($39.0 \leq X \geq 31.0$) and negatively with COR, CON, and ENT in both muscles.

Kamruzzaman *et al*. (2013) reported in cooked lamb meat that textural parameters based on WBSF, image texture features such as COR and CON were positively correlated with roughness ($WBSF \geq 45$ N) and negatively for tenderness ($WBSF \leq 45$ N). On the other hand,

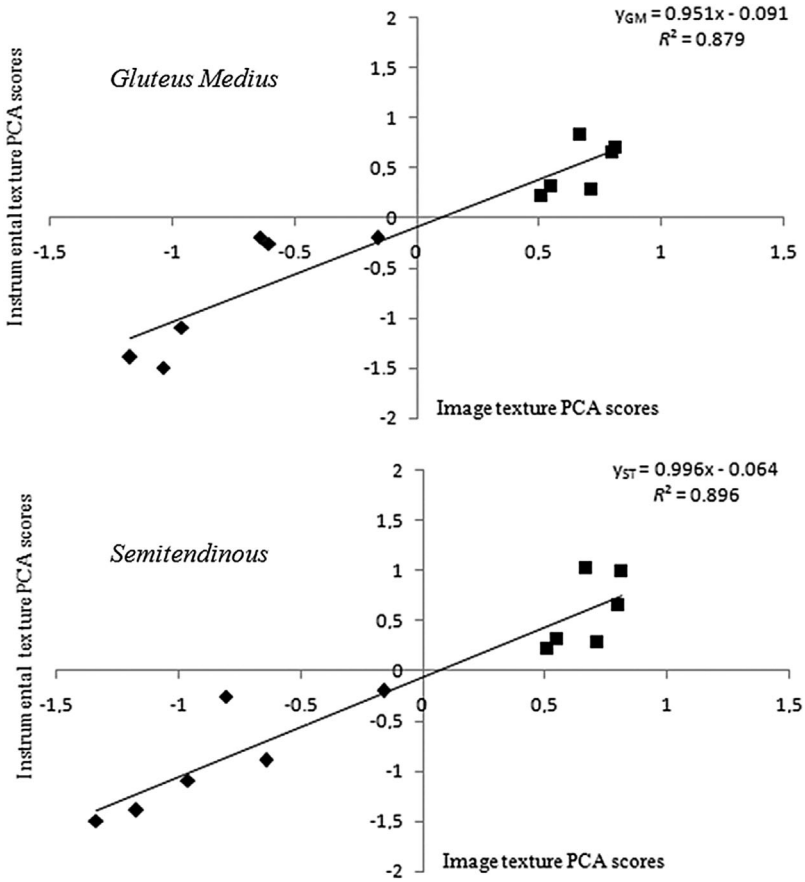

Fig 3. Correlation coefficients of PCA scores between instrumental texture versus image texture of cooked (◆) and cooked freeze dried rehydrated (■) *Semitendinous* (ST) and *Gluteus Medius* (GM) bovine muscle.

ASM and HOM were positively correlated for tenderness and negatively for toughness.

Jeyamkondan *et al*. (2001) explored textural features based on the GLCM to predict tenderness in meat. Instead of GLCM-based features, they chose to extract features derived from the gray-level difference histogram. Results revealed that image texture features extracted from the full images predicted WBSF scores with an R^2 value of 0.5 and correctly classified the steaks into categories of "tenderness" and "toughness" with a 79% success rate. Features extracted from the close-up images predicted WBSF scores with an R^2 value of 0.72 and classified the steaks with a 92% success rate.

Among these texture features evaluated, tender samples in ST and GM always showed negative correlation with CON, ENT, and COR features and positive correlation with ASM and HOM. Overall, these results suggested that the texture features extracted from images analysis could be very useful to evaluate tenderness.

Conclusions

An imaging-based technique was developed to approach texture properties in *Semitendinous* and *Gluteus Medius* bovine muscles for instant meal. Magnification at 1,000× showed to be the best option to evaluate image texture due to that image texture analysis performed at 1,000× by gray level co-occurrence matrix had high correlations with instrumental texture features when compared to lower magnifications. On the other hand, images of meat surface allowed classifying meat in terms of texture—characterized by tenderness.

These results suggest the relevance of image analysis, due to that prediction of texture and tenderness in meat can be performed easily as a quantitative and non-invasive technique that could be related in future studies for quality in bovine muscles. Anyway, it would be recommendable to investigate other magnifications in future research in order to establish a general trend and other bovine muscles should be evaluated to improve research.

Reference

Basset O, Buquet B, Abouelkaram S, Delachartre P, Culioli J. 2000. Application of texture image analysis for the classiffcation of bovine meat. Food Chem 69:437–445.

Belew J, Brooks J, McKenna R, Savell J. 2003. Warner–Bratzler shear evaluations of 40 bovine muscles. Meat Sci 64:507–512.

Chen L, Opara U. 2013. Texture measurement approaches in fresh and processed foods—a review. Food Res Int 51:823–835.

ElMasry G, Sun D, Allen P. 2012. Near-infrared hyperspectral imaging for predicting colour, pH and tenderness of fresh beef. J Food Eng 110:127–140.

Guzek D, Głąbska D, Pogorzelska E, Pogorzelski G, Wierzbick A. 2013. Instrumental measurement of meat in a laboratory research and on a production line. Adv Sci Technol Res J 7:5–11.

Jackman P, Sun D, Du C, Allen P. 2009. Prediction of beef eating qualities from colour, marbling and wavelet surface texture features using homogenous carcass treatment. Pattern Recogn 42:751–763.

Jackman P, Sun D. 2013. Recent advances in image processing using image texture features for food quality assessment. Trends Food Sci Tech 29:35–43.

Jeyamkondan S, Kranzler G, Lakshmikanth A. 2001. Predicting beef tenderness with computer vision. Can Ag Eng 300:1–10.

Juarez M, Aldai N, Lopez-Campos O, Dugan M, Uttaro B, Aalhus J. 2012. Beef texture and juiciness. In: Hui YH, editor. Handbook of meat and meat processing. Boca Raton, Florida: CRC Press.

Kamruzzaman M, ElMasry G, Sun D, Allen P. 2013. Non-destructive assessment of instrumental and sensory tenderness of lamb meat using NIR hyperspectral imaging. Food Chem 141:389–396.

Karimi M, Fathi M, Sheykholeslam Z, Sahraiyan B, Naghipoor F. 2012. Effect of different processing parameters on quality factors and image texture features of bread. J Bioproces Biotech 2:2–7.

Kong F, Tang J, Lin M, Rasco B. 2008. Thermal effects on chicken and salmon muscles: tenderness, cook loss, area shrinkage collagen solubility and microstructure. LWT Food Sci Technol 41:1210–1222.

Kono S, Kawamura I, Yamagami S, Araki T, Sagara Y. 2014. Optimum storage temperature of frozen cooked rice predicted by ice crystal measurement, sensory evaluation and artificial neural network. Int J Refrig 56:165–172.

Laddi A, Sharma S, Kumar A, Kapur P. 2013. Classification of tea grains based upon image texture feature analysis under different illumination conditions. J Food Eng 115:226–231.

Lawless H, Heymann H. 1998. Sensory evaluation of food: principals and practices. New York: Chapman and Hall.

Leelayuthsoontorn P, Thipayarat A. 2006. Textural and morphological changes of Jasmine rice under various elevated cooking conditions. Food Chem 96:606–613.

Luckett C, Kuttappan V, Johnson L, Owens C, Seo H. 2014. Comparison of three instrumental methods for predicting sensory attributes of poultry deli meat. J Sens Stud 29: 171–181.

Mendoza F, Lu R, Diwan A, Cen H, Bailey B. 2012. Integrated spectral and image analysis of hyperspectral scattering data for prediction of apple fruit firmness and soluble solids content. Postharvest Biol and Tech 62:149–160.

Messina V, Sancho A, Grigioni G, Filipini S, Pazos A, Paschetta F, Chamorro V, Walsoe de Reca N. 2014. Evaluation of different bovine muscles to be applied in freeze drying for instant meal. Study of physicochemical and senescence parameters. J Animal 9:723–772.

Meullenet J, Gross J, Marks B, Daniels M. 1998. Sensory descriptive texture analyses of cooked rice and its correlation to instrumental parameters using a extrusion cell. Cereal Chem 75:714–720.

Mounir S. 2015. Texturing of chicken breast meat as an innovative way to intensify drying: use of a coupled washing/diffusion cwd phenomenological model to enhance kinetics and functional properties. Dry Technol 33:1369–1381.

Oikonomopoulou V, Krokida M, Karathanos V. 2011. The influence of freeze drying conditions on microstructural changes of food products. Procedia Food Sci 1:647–654.

Ou X, Pan W, Xiao P. 2014. In vivo skin capacitive imaging analysis by using grey level co-occurrence matrix (GLCM). Int J Pharm 460:28–32.

Reyes A, Perez N, Mahn A. 2011. Theoretical and experimental study of freeze −drying "loco" (Concholepas concholpeas). Dry Technol 29:1386–1395.

Rust S, Price D, Subbiah J, Kranzler G, Hilton G, Vanoverbeke D, Morgan J. 2008. Predicting beef tenderness using near-infrared spectroscopy. J Anim Sci 86:211–219.

Saini M, Singh J, Prakash N. 2014. Analysis of wheat grain varieties using image processing—a review. IJSR 3:490–495.

Sullivan G, Calkins C. 2011. Ranking beef muscles for Warner–Bratzler Shear force and trained sensory panel ratings from published literature. J Food Quality 34:195–203.

Sun X, Chen K, Maddock-Carlin K, Anderson V, Lepper A, Schwartz C, Keller W, Ilse B, Magolski J, Berg E. 2012. Predicting beef tenderness using color and multispectral image texture features. Meat Sci 92:386–393.

Wezemael L, De Smet S, Ueland O, Verbeke W. 2014. Relationships between sensory evaluations of beef tenderness, shear force measurements and consumer characteristics. Meat Sci 97:310–315.

Yang X, Beyenal H, Harkin G, Lewandowski Z. 2000. Quantifying biofilm structure using image analysis. J Microbiol Meth 39:109–119.

Zheng C, Sun D, Zheng L. 2006. Recent applications of image texture for evaluation of food qualities—a review. Trends Food Sci Tech 17:113–128.